HHS Public Access
Author manuscript
Min Eng. Author manuscript; available in PMC 2018 May 17.

Published in final edited form as:
Min Eng. 2018 May ; 70(5): 69–74. doi:10.19150/me.8238.

Dust control by air-blocking shelves and dust collector-to-bailing airflow ratios for a surface mine drill shroud

Y. Zheng, **W.R. Reed**, **J.D. Potts**, **M. Li**, and **J.P. Rider**
Associate service fellow, mining engineer, branch chief, mining engineer and acting team leader, respectively, at the Centers for Disease Control and Prevention, National Institute for Occupational Safety and Health (CDC NIOSH), Pittsburgh, PA, USA

Abstract

The National Institute for Occupational Safety and Health (NIOSH) recently developed a series of validated models utilizing computational fluid dynamics (CFD) to study the effects of air-blocking shelves on airflows and respirable dust distribution associated with medium-sized surface blasthole drill shrouds as part of a dry dust collector system. Using validated CFD models, three different air-blocking shelves were included in the present study: a 15.2-cm (6-in.)-wide shelf; a 7.6-cm (3-in.)-wide shelf; and a 7.6-cm (3-in.)-wide shelf at four different shelf heights. In addition, the dust-collector-to-bailing airflow ratios of 1.75:1, 1.5:1, 1.25:1 and 1:1 were evaluated for the 15.2-cm (6-in.)-wide air-blocking shelf. This paper describes the methodology used to develop the CFD models. The effects of air-blocking shelves and dust collector-to-bailing airflow ratios were identified by the study, and problem regions were revealed under certain conditions.

Introduction

Surface blasthole drilling can generate considerable amounts of respirable silica dust. These high dust concentrations can be exacerbated by the high silica content as drilling cuts through silica-bearing materials such as sandstone and shale, causing overexposures for miners to respirable silica dust. These overexposures can lead to silicosis, an occupational lung disease that has no cure and is often fatal. A review of the Mine Safety and Health Administration (MSHA) respirable silica dust sample database from 2010 to 2016 for metal/nonmetal mining shows the following overexposure rates for occupations related to blasthole drilling:

- 14.1 percent of rotary air drillers were overexposed to respirable silica dust (22 out of 156 samples).
- 5.8 percent of rotary drillers were overexposed to respirable silica dust (nine out of 155 samples).
- 7.3 percent of drill helpers were overexposed to respirable silica dust (three out of 41 samples).

Disclaimer
The findings and conclusions in this manuscript are those of the authors and do not necessarily represent the views of NIOSH. Mention of company names or products does not constitute endorsement by NIOSH.

- 7.5 percent of blasters/shotfirers were overexposed to respirable silica dust (three out of 40 samples).

Of significant interest is an X-ray surveillance study recently completed under the National Institute for Occupational Safety and Health (NIOSH) Enhanced Coal Workers' Health Surveillance Program. This program offered free chest radiographs to surface coal miners in 16 states. Pneumoconiosis was found in 2 percent of the 2,328 screened miners with at least one year of mining tenure. Twelve miners had radiographic changes consistent with progressive massive fibrosis, and nine of these 12 miners reported no underground mining tenure. All but one of the nine miners worked at occupations that were in the vicinity of blast-hole drilling, either as a driller, blaster or blast crew member (Halldin et al., 2015).

Many rotary blasthole drilling operations use a dry collection system (Cecala et al., 2012). Although wet drilling is a better dust control method, it requires a constant water supply, reducing drill bit life through excessive bearing wear and hydrogen embrittlement, and causing freezing-related issues in colder climates.

For medium-sized and large drills, such as the Atlas Copco DM45, Sandvik 460 and Drilteck D45K, a typical dry dust collection system schematic is shown in Fig. 1. Many studies have been completed on dry dust collectors, so a detailed operational description will not be provided here (Maksimovic and Page, 1985; Bailey and Page, 1987; Organiscak and Page, 1995; Organiscak and Page, 2005; Reed et al., 2008; Potts and Reed, 2008, 2011). To summarize the collector operation, compressed air (bailing air) is used to flush the drill cuttings out of the drillhole. The exhaust fan on the collector body is used to pull dusty air and material from the drill shroud into the collector housing where it is filtered.

This study focuses on the drill shroud portion of the dust collector. In order to understand the respirable dust behavior in and around the drill shroud and to develop and evaluate the effectiveness of various control techniques, numerical simulations using computational fluid dynamics (CFD) can be applied to evaluate different scenarios. In order to ensure the correctness of the CFD modeling, previously run experiments conducted in the NIOSH full-scale drill shroud laboratory were utilized to validate the CFD models. Simulation results were compared with the experimental data for a 0.14-m^3/s (300-cfm) and a 0.24-m^3/s (500-cfm) bailing airflow with 2:1, 3:1 and 4:1 dust collector-to-bailing airflow ratios, having a 5.0-cm (2-in.) gap at the shroud-to-ground interface, which is a commonly encountered gap size for medium-sized rotary blasthole drill. The comparison was made evaluating dust concentrations generated from the drill shroud in the laboratory to those predicted from the simulations. For the CFD simulations conducted using 2:1 and 3:1 ratios, results showed that these models could accurately predict dust generated from laboratory conditions (Zheng et al., 2016).

The experimental data (Page and Organiscak, 2004; Page, Reed and Listak, 2008) and CFD simulation results (Zheng et al., 2016) indicate that the dusty bailing airflow leakage can be greatly reduced when the dust collector-to-bailing airflow ratio increases to 4:1, with a 5.0-cm (2-in.) gap. However, this 4:1 ratio is far more than the common dry dust collector's capacity, which typically provides a 2:1 dust collector-to-bailing airflow ratio (Page, Reed and Listak, 2008).

Author Manuscript

Author Manuscript

Author Manuscript

To reduce the dusty air leakage due to the Coanda effect, it is desirable to eliminate or weaken the Coanda effect at least near the shroud-to-ground gap area. An air-blocking shelf was introduced in the mining industry to reduce the dust emissions, and it demonstrated about 70 to 81 percent dust reduction in the field and in the laboratory (Potts and Reed, 2008, 2011).

In the present study, CFD simulations are used to reveal the effectiveness of air-blocking shelves. Three different air-blocking shelves were included in this study: a 15.2-cm (6-in.)-wide shelf; a 7.6-cm (3-in.) wide-shelf; and a 7.6-cm (3-in.)-wide shelf at four different heights. The evaluation is based on the CFD-validated models from a previous 0.24-m^3/s (500-cfm) bailing airflow with a 2:1 dust collector-to-bailing airflow ratio and a 5.1-cm (2-in.) shroud-to-ground gap. The 15.2-cm (6-in.)-wide air-blocking shelf is further evaluated with the dust collector-to-bailing airflow ratios of 1.75:1, 1.5:1, 1.25:1, and 1:1 to assess the value of the ratios with the combination of the air-blocking shelf.

CFD modeling

The ANSYS Fluent Version 15.0 program (ANSYS Inc., Canonsburg, PA) was used to perform the analysis of dust distribution in this paper. Using the software drawing tools provided by ANSYS, the schematic of the airflow domain inside the drill table simulator was built according to the geometry measured from the full-sized facility. The facility has been fully described in previous literature (Organiscak and Page, 2005; Page, Reed and Listak, 2008; Potts and Reed, 2008; Reed and Potts, 2010).

A schematic of the computational domain for the three different air-blocking shelves is shown in Fig. 2. The geometric models considered in this study were:

- 15.2-cm (6-in.)-wide air-blocking shelf (Fig. 2a).
- 7.6-cm (3-in.)-wide air-blocking shelf (Fig. 2b).
- 7.6-cm (3-in.)-wide air-blocking shelf at four different heights (Fig. 2c).

The boundary conditions applied in the simulation are illustrated in Fig. 2a. Fresh airflow is pulled into the simulation domain through the three openings on the roof, shown as roof airflow inlets in Fig. 2a. This airflow compensates for the difference in airflow between the dust collector flow and the bailing airflow, which are set according to the different collector-to-bailing airflow ratios. The dust collector outlet is the only outlet in the simulation domain to allow airflow to exit the laboratory domain. The bailing airflow, together with the roof airflow, enter the domain at the same time. The bailing air with dust is injected into the simulation domain from a circular face inside the hollow drill pipe, as indicated by the bailing air inlet in Fig. 2a.

For all of the simulation cases, the respirable dust concentrations are collected at the four samplers' locations, as indicated in Fig. 2a. For both of the simulations with the air-blocking shelf at one level, the shelf is positioned inside the shroud at two-thirds the total shroud height, which is 81.3 cm (32 in.) above the ground. For the third case with the air-blocking shelf at four different heights, the shelf sides have a 15.2-cm (6-in.) increase in height, starting at the dust collector side and progressing counter-clockwise toward the back of the test facility, with the lowest shelf at 50.8 cm (20 in.) above the ground with no overlap of the shelf vertically, as shown in Fig. 2c.

Previously validated CFD models were used in this study to evaluate the effect of an air-blocking shelf on dust control. Dust was treated as a gas — carbon dioxide (CO_2) — and a species transport model in Fluent was used. The CFD software uses the steady-state Navier-Stokes equations, continuity equations, and conservation of energy equations as the basic equations to resolve computer models. The mixture properties are derived using incompressible ideal gas law within the simulation domain, which is 3.66 m wide by 3.05 m deep by 2.44 m high (12 × 10 × 8 ft). Turbulence was modeled using the realizable K-epsilon turbulence model with enhanced wall treatment.

In order to ensure simulation accuracy, mesh generation was completed by ensuring high cell density near the drill pipe, at the ground-to-shroud gap, and in the bounding wall regions where high gradients exist. During mesh generation, the EquiSize Skew was monitored and maintained at a value less than 0.85. Cells with skewness of 0.90 or more may cause problems with the model results by preventing solution convergence, thus producing inaccurate solutions.

The boundary conditions used to determine the dust distribution inside the NIOSH full-scale drill shroud laboratory are listed in Table 1. The inputs for roof airflow inlet and bailing air inlet are calculated specifically to the test facility dimensions and the desired collector-to-bailing airflow ratios.

Characteristics of airflow and dust underneath the drill shroud

Effect of different air-blocking shelves

The airflow patterns and dust control capabilities were simulated for the three types of air-blocking shelves. They were evaluated under the same ventilation conditions: 0.24 m^3/s (500 cfm) of bailing airflow, 0.24 m^3/s (500 cfm) of fresh roof airflow, and 0.48 m^3/s (1,000 cfm) of dust air mixture collected by the dust collector outlet, which equates to a 2:1 collector-to-bailing airflow ratio.

It can be observed from Fig. 3a that after the dusty air is released from the bailing air inlet, it travels down inside the hollow drill stem, then makes a 180° turn up the gap between the drill steel and drill hole. As the high-velocity air flows up, it follows the outside surface of the drill steel and encounters the underside of the drill deck, where it fans out in all directions and continues to follow the inner shape of the shroud down to where the air-blocking shelf is located.

After the flow encounters the 15.2-cm (6-in.)-wide air-blocking shelf, the CFD simulation shows that most of the flow goes horizontally toward the drill steel and then follows the upward bailing air and repeats the pattern while it continues to be drawn in by the dust collector. At the same time, some of the dusty air travels below the air-blocking shelf, where it mixes with fresh airflow that is drawn into the drill shroud through the 5.1-cm (2-in.)

shroud-to-ground gap. The dusty bailing airflow underneath the air-blocking shelf shows a complicated three-dimensional flow pattern due to the combined forces from the dust collector and incoming fresh airflow, but cannot escape under the current conditions outside of the drill shroud.

It can be observed from Fig. 3a that the air-blocking shelf hinders the flow of air traveling down the inside wall of the vertical drill shroud and prevents it from directly striking the ground. The airflow above the air-blocking shelf shows a strong Coanda effect, where the airflow tends to attach to nearby surfaces (Trancossi, 2011), while the airflow below the air-blocking shelf does not show any apparent Coanda effect.

Previous studies (Potts and Reed, 2008, 2011; Zheng et al., 2016) showed that the Coanda effect causes the dusty bailing air to strike the ground and leak out from the shroud-to-ground gap in the vicinity. The air-blocking shelf effectively eliminates the Coanda effect at the shroud-to-ground gap area. As a result, the respirable dust is confined inside the drill shroud, as clearly indicated in Fig. 3b, and the miners working nearby should not be exposed to respirable dust from the drill should.

The flow pattern for the 7.6-cm (3-in.)-wide air-blocking shelf is shown in Fig. 4a. The main difference in comparison to the 15.2-cm (6-in.)-wide air-blocking shelf is that there is not a strong horizontal airflow after the bailing air encounters the 7.6-cm (3-in.)-wide air-blocking shelf. In this case, most of the bailing air is diverted toward the lower center of the shroud below the air-blocking shelf. This change in airflow direction diverts the airflow and it strikes the ground away from the vertical walls of the drill shroud, making the dust harder to escape the shroud.

As shown in Fig. 4a, airflows traveling down the vertical shroud walls hit the air-blocking shelf, reducing the force of the bailing air that strikes the ground and allowing the respirable dust to be confined inside the shroud, as shown in Figs. 4a and 4b.

The flow pattern for the 7.6-cm (3-in.)-wide air-blocking shelf at four levels is shown in Fig. 5. As mentioned earlier, the four shelves attached to the vertical walls had a 15.2-cm (6-in.) increase in height without overlapping vertically. This arrangement can allow the flexibility of the shelf construction to avoid some structure restrictions. The height differences and air-blocking shelf pattern were randomly selected as an example.

The results from the CFD simulation in Fig. 5a show that pathlines of bailing airflow have similar flow patterns as the 7.6-cm (3-in.)-wide air-blocking shelf. Due to the width of this air-blocking shelf, it cannot produce strong horizontal flow after the bailing air hits the shelf, as was observed with the 15.2-cm (6-in.)-wide air-blocking shelf. However, it still can divert the bailing airflow direction toward the center region of the shroud and reduce the striking ground force, even when there is still some airflow adhering to the shroud's vertical walls below the air-blocking shelf.

This arrangement of air-blocking shelves at different levels can still effectively confine the respirable dust under the 2:1 collector-to-bailing airflow ratio and the 5.1-cm (2-in.) shroud-to-ground gap condition. As shown in Figs. 5a and 5b, dust does not leak out of the shroud to pollute the surroundings.

Simulation with different dust collector-to-bailing airflow ratios

At a 2:1 dust collector-to-bailing airflow ratio, the CFD simulation revealed that the three types of air-blocking shelves were able to effectively confine the respirable dust inside the drill shroud. However, in a previous study it was shown that the dust collector-to-bailing airflow ratio was also a critical parameter (Zheng et al., 2016). In this section, the effect of an air-blocking shelf under different dust collector-to-bailing airflow ratios is evaluated to investigate whether the ratio is still an important factor.

Using the 15.2-cm (6-in.)-wide air-blocking shelf, dust control efficiencies were evaluated under different dust collector-to-bailing airflow ratios. The bailing airflows were kept the same as shown in Table 1, while the fresh roof airflow was calculated to be 0.18 m^3/s (375 cfm), 0.12 m^3/s (250 cfm), 0.06 m^3/s (125 cfm) and 0 m^3/s (0 cfm) to represent the collector-to-bailing airflow ratios of 1.75:1, 1.5:1, 1.25:1 and 1:1, respectively.

It can be observed in Fig. 6a that the CFD simulation for the 1.75:1 ratio showed the bailing airflow pattern was very similar to the 2:1 ratio case shown in Fig. 3. Most of the bailing airflow is diverted horizontally toward the drill steel after it strikes the air-blocking shelf, while some of the dusty bailing air goes below the air-blocking shelf but rarely touches the ground. Several pathlines travel close to the 5.1-cm (2-in.) shroud-to-ground gap, but are drawn back to the dust collector by the incoming fresh airflow. The dust distribution as shown in Fig. 7a is totally confined inside the drill shroud for the 1.75:1 ratio case.

When the dust-collector-to-bailing airflow ratio is reduced to 1.5:1, as shown in Fig. 6b, it can be seen that some pathlines start to escape out of the drill shroud at the regions far away from the opening of the dust collector. Due to the decrease in the dust collector-to-bailing airflow ratio, more dusty bailing air is circulating below the air-blocking shelf and has more of a chance to leak out. The lack of inward airflow at the shroud-to-ground gap, which forces the dusty air away from the shroud-to-ground gap opening, causes leakage at those areas. As a result, as shown in Fig. 7b, respirable dust escapes outside of the shroud and pollutes the surrounding work region.

As the collector-to-bailing airflow decreases, more dusty bailing airflow leaks out as less airflow is drawn in, as shown in Fig. 6c for the 1.25:1 collector-to-bailing airflow ratio. At a 1:1 collector-to-bailing airflow ratio, no fresh air flows into the shroud, as shown in Fig. 6d. The flow patterns for Figs. 6c and 6d indicate that the leakage starts at the furthest region away from the dust collector side, but interestingly, these leakage airflows are drawn back inside the drill shroud on the dust collector inlet side. As shown in Figs. 7b, 7c and 7d, respirable dust has leaked outside the drill shroud.

Conclusion

This study evaluated the dust control capability of three types of air-blocking shelves with different widths and installations. It was found that all three air-blocking shelves can effectively confine the respirable dust inside the drill shroud with no dust leakage under the conditions of a 2:1 dust collector-to-bailing airflow ratio and a 5.1-cm (2-in.) shroud-to-ground gap. The study was based on a previously validated CFD model.

From the study, it can be observed that the air-blocking shelf can effectively eliminate or greatly reduce the Coanda effect below the shelf and reduce the strike force of the dusty bailing airflow near the shroud-to-ground gap. At the same time, dust collector-to-bailing airflow ratios are still critical factors in drill shroud dust control. Even with an air-blocking shelf, a low dust collector-to-bailing airflow ratio can still cause serious dust leakage, such as dusty bailing airflow that can freely escape the shroud-to-ground gap without striking the ground. From this study, it is estimated that a dust collector-to-bailing airflow ratio of at least 1.75:1 needs to be maintained with an air-blocking shelf to effectively confine dust. Without an air-blocking shelf, the same control effect can only be achieved above a 4:1 dust collector-to-bailing airflow ratio, as revealed previously.

This study can provide guidelines for a mining engineer to fully understand the dust problem for the drilling jumbo and drill shroud. From this study, it is highly recommended to install an air-blocking shelf and maintain the dust collector-to-bailing airflow ratio to protect the miners in the vicinity of affecting areas.

Acknowledgments

The authors of this paper sincerely acknowledge Jay F. Colinet, John A. Organiscak, Timothy W. Beck, and Liming Yuan for their technical support. The authors also thank Jason S. Driscoll, Milan R. Yekich, and Andrew L. Mazzella for their help with experimental and facility measurement.

References

Bailey, BPJ., Page, SJ. Agglomeration of Collected Drill Dust. 1987. USBM Contract No SO368000

Cecala, AB., O'Brien, AD., Schall, J., Colinet, JF., Fox, WR., Franta, RJ., Joy, J., Reed, WR., Reeser, PW., Rounds, JR., Schultz, MJ. Dust control handbook for industrial minerals mining and processing. U.S. Department of Health and Human Services, Centers for Disease Control and Prevention National Institute for Occupational Safety and Health; 2012. p. 284DHHS DHHS(NIOSH) Publication No. 2012-112, Report of Investigations 9689https://www.cdc.gov/niosh/mining/works/coversheet1765.html

Halldin CN, Reed WR, Joy GJ, Colinet JF, Rider JP, Petsonk EL, Abraham JL, Wolfe AL, Storey E, Laney AS. Debilitating lung disease among surface coal miners with no underground mining tenure. Journal of Occupational and Environmental Medicine. 2015; 57(1):62–67. https://doi.org/10.1097/jom.0000000000000302. [PubMed: 25563541]

Maksimovic SD, Page SJ. Quartz Dust Sources During Overburden Drilling at Surface Coal Mines. US Bureau of Mines Information Circular 9056. 1985 Jan.

Organiscak, JA., Page, SJ. Assessment of airborne dust generated from small truck-mounted rock drills; US Bureau of Mines Report of Investigations 9616. 1995. p. 17https://www.cdc.gov/niosh/nioshtic-2/00233930.html

Organiscak JA, Page SJ. Development of a dust collector inlet hood for enhanced surface mine drill dust capture. International Journal of Surface Mining, Reclamation & Environment. 2005; 19(1): 12–28. https://doi.org/10.1080/13895260412331314248.

Page SJ, Organiscak JA. Semi-empirical model for predicting surface coal mine drill respirable dust emissions. International Journal of Surface Mining, Reclamation, and Environment. 2004; 18(1): 42–59. https://doi.org/10.1076/ijsm.18.142.23546.

Page SJ, Reed R, Listak JM. An expanded model for predicting surface coal mine respirable dust emissions. International Journal of Mining, Reclamation, and Environment. 2008; 22(3):210–221. https://doi.org/10.1080/17480930701828833.

Potts JD, Reed WR. Horizontal air blocking shelf reduces dust leakage from surface drill shroud. Transactions of the Society for Mining, Metallurgy & Exploration. 2008; 324:55–60.

Potts JD, Reed WR. Field evaluation of air-blocking shelf for dust control on blasthole drills. International Journal of Surface Mining, Reclamation, and Environment. 2011; 25(1):32–40. https://doi.org/10.1080/17480930.2011.540376.

Reed W, Listak J, Page S, Organiscak J. Summary of NIOSH research completed on dust control methods for surface and underground drilling. Transactions of the Society for Mining, Metallurgy & Exploration. 2008; 324:32–40.

Reed WR, Potts JD. Improved drill shroud capture of respirable dust utilizing air nozzles underneath the drill deck. Transactions of the Society for Mining, Metallurgy & Exploration. 2010; 326:10–15.

Trancossi, M. An Overview of Scientific and Technical Literature on Coanda Effect Applied to Nozzles. 2011. SAE Technical Paper 2011-01-2591https://doi.org/10.4271/2011-01-2591

Zheng Y, Reed WR, Zhou L, Rider JP. Computational fluid dynamics modeling of a medium-sized surface mine blasthole drill shroud. Mining Engineering. 2016; 68(11):43–49. https://doi.org/10.19150/me.6831. [PubMed: 27932851]

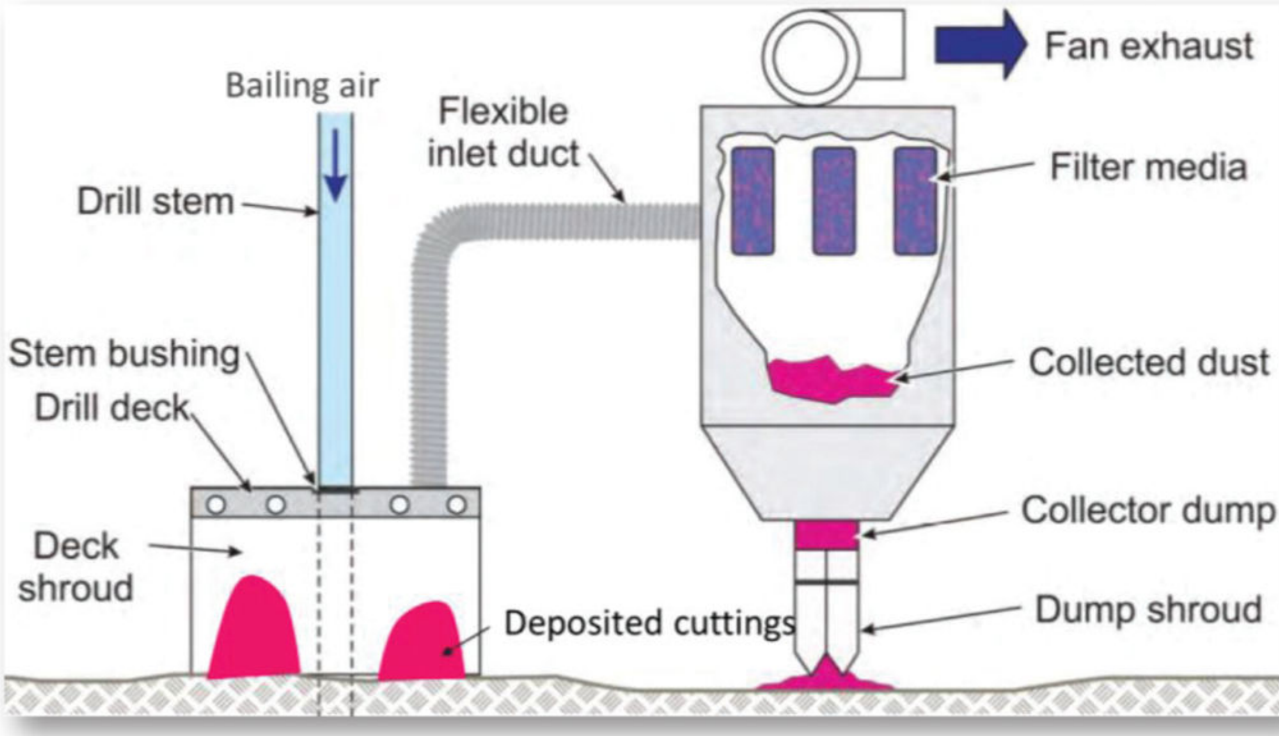

Figure 1.
A basic dry dust collection system on a drill.

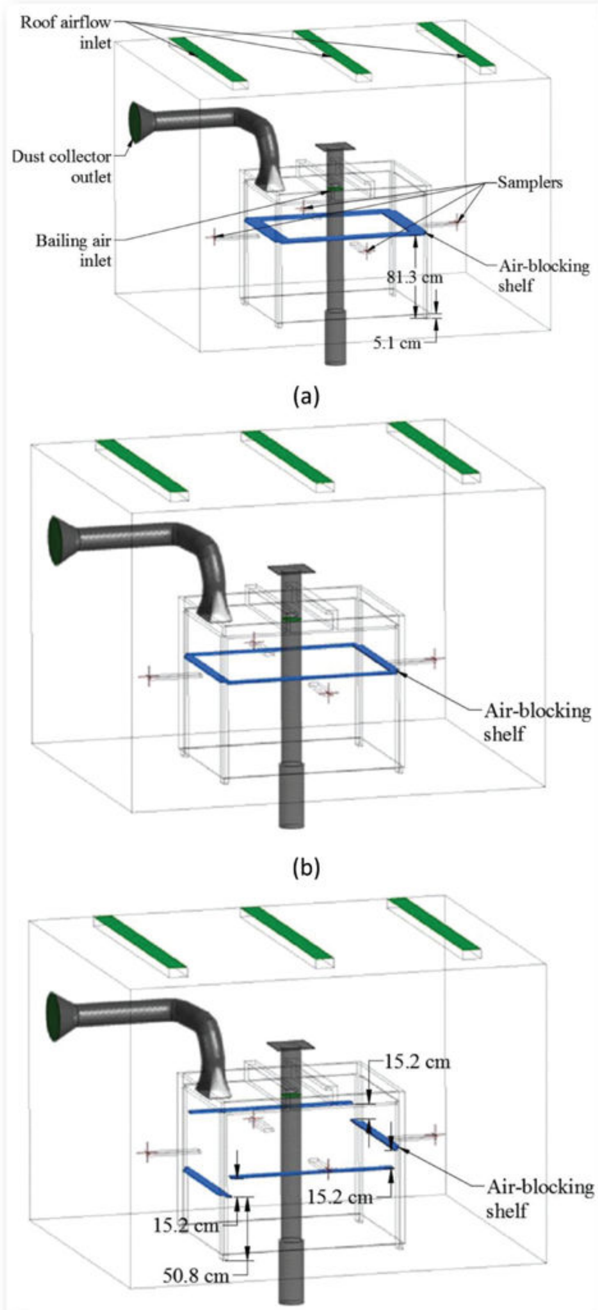

Figure 2.

Overview of the CFD model with boundary conditions for (a) 15.2-cm (6-in.)-wide air-blocking shelf, (b) 7.6-cm (3-in.)-wide air-blocking shelf, and (c) 7.6-cm (3-in.)-wide air-blocking shelf at four levels.

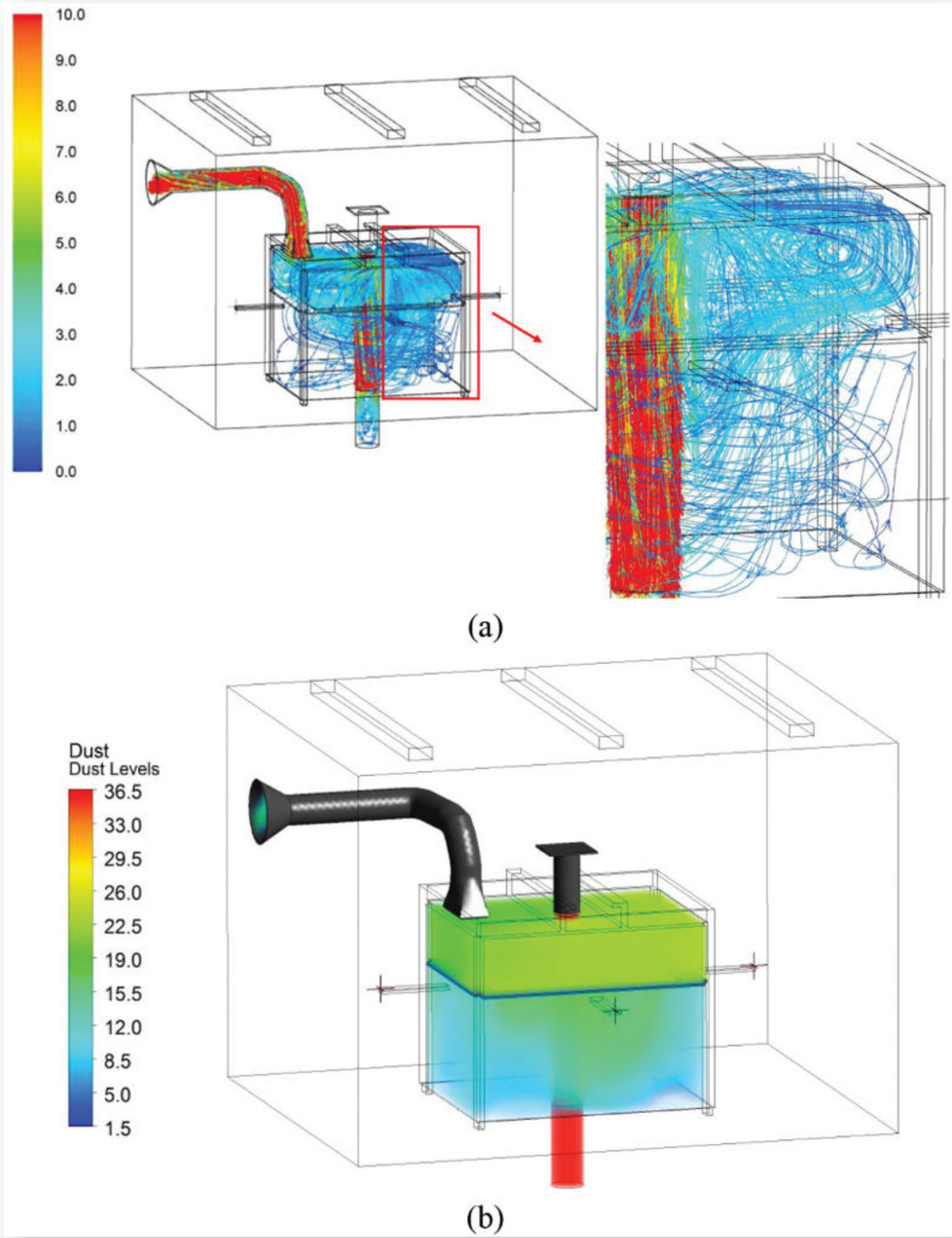

Figure 3.

(a) Pathlines of bailing airflow colored by velocity magnitude (0.0 to 10.0 m/s) (b) Respirable dust concentration distributions. Legend shows the dust levels (1.5 to 36.5 mg/m^3) with a 15.2-cm (6-in.)-wide air-blocking shelf and a dust collector-to-bailing airflow ratio of 2:1.

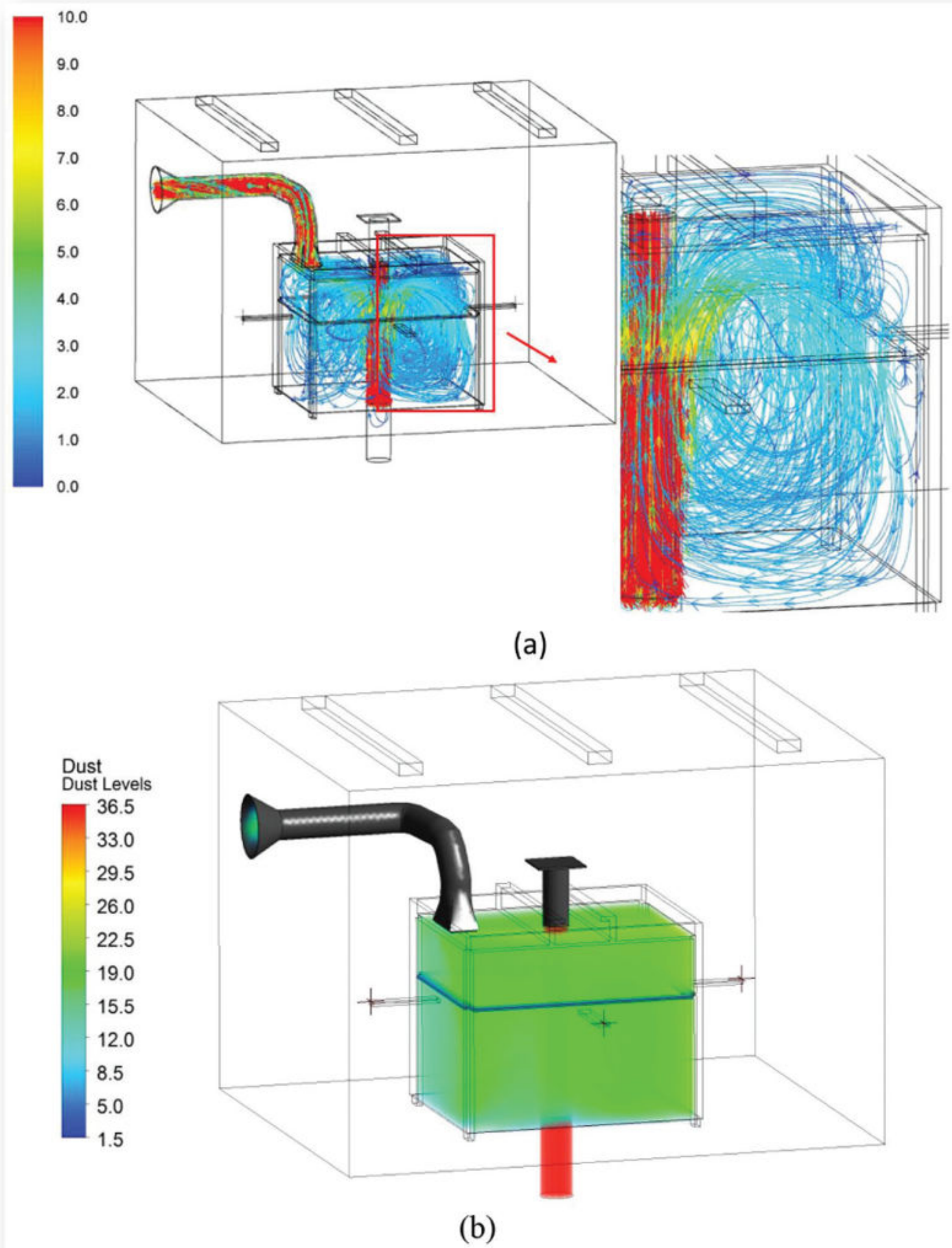

Figure 4.

(a) Pathlines of bailing airflow colored by velocity magnitude (0.0 to 10.0 m/s) (b) Respirable dust concentration distributions. Legend shows the dust levels (1.5 to 36.5 mg/m^3) with a 7.6-cm (3-in.)-wide air-blocking shelf and a dust collector-to-bailing airflow ratio of 2:1.

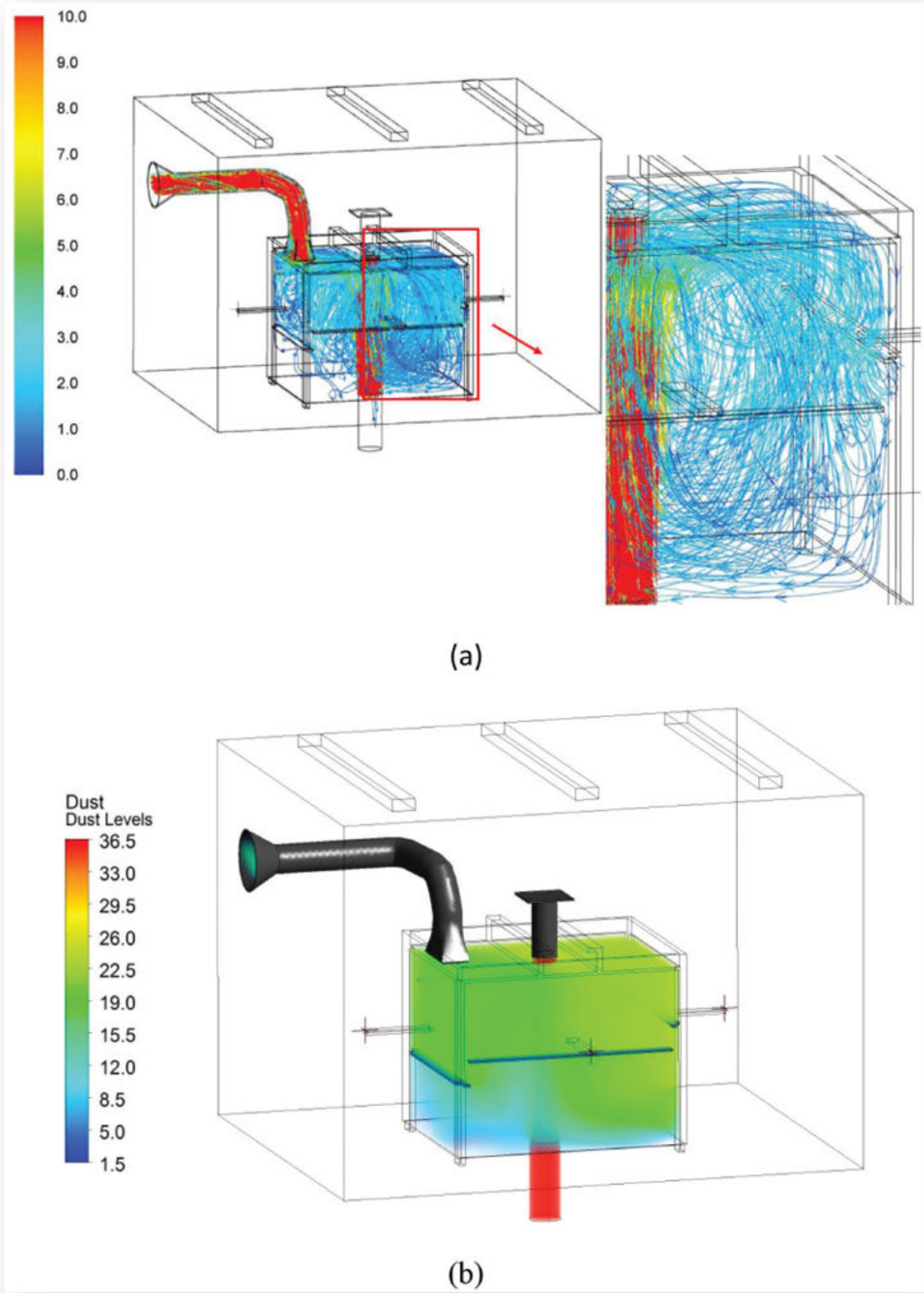

Figure 5.
(a) Pathlines of bailing airflow colored by velocity magnitude (0.0 to 10.0 m/s) (b) Respirable dust concentration distributions. Legend shows the dust levels (1.5 to 36.5 mg/m^3) with a 7.6-cm (3-in.)-wide air-blocking shelf at four levels and a dust-collector-to-bailing airflow ratio of 2:1.

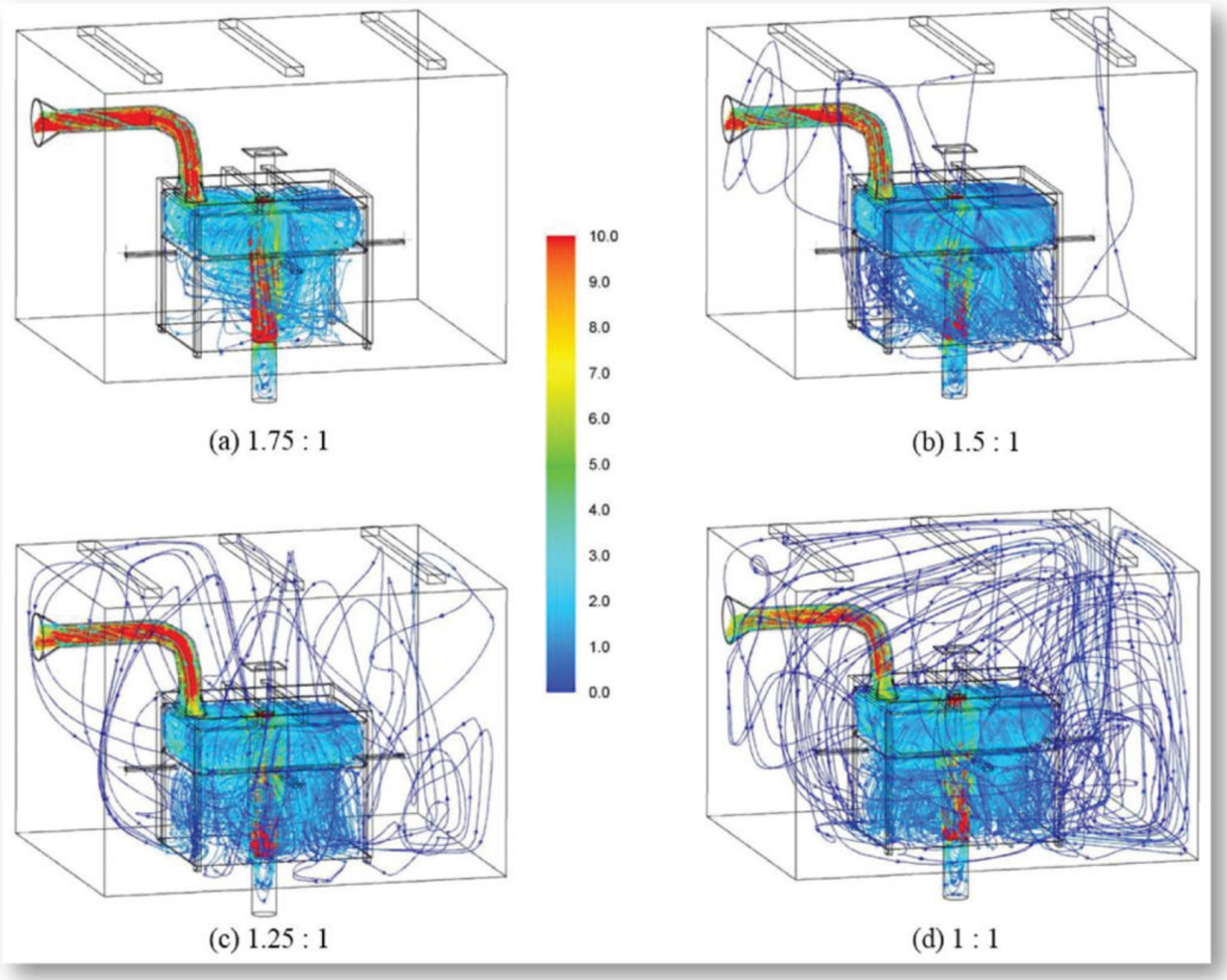

Figure 6.

Pathlines of bailing airflow colored by velocity magnitude (0.0 to 10.0 m/s) with 15.2-cm (6-in.)-wide air-blocking shelves for different dust-collector-to-bailing airflow ratios: (a) 1.75:1, (b) 1.5:1, (c) 1.25:1 and (d) 1:1.

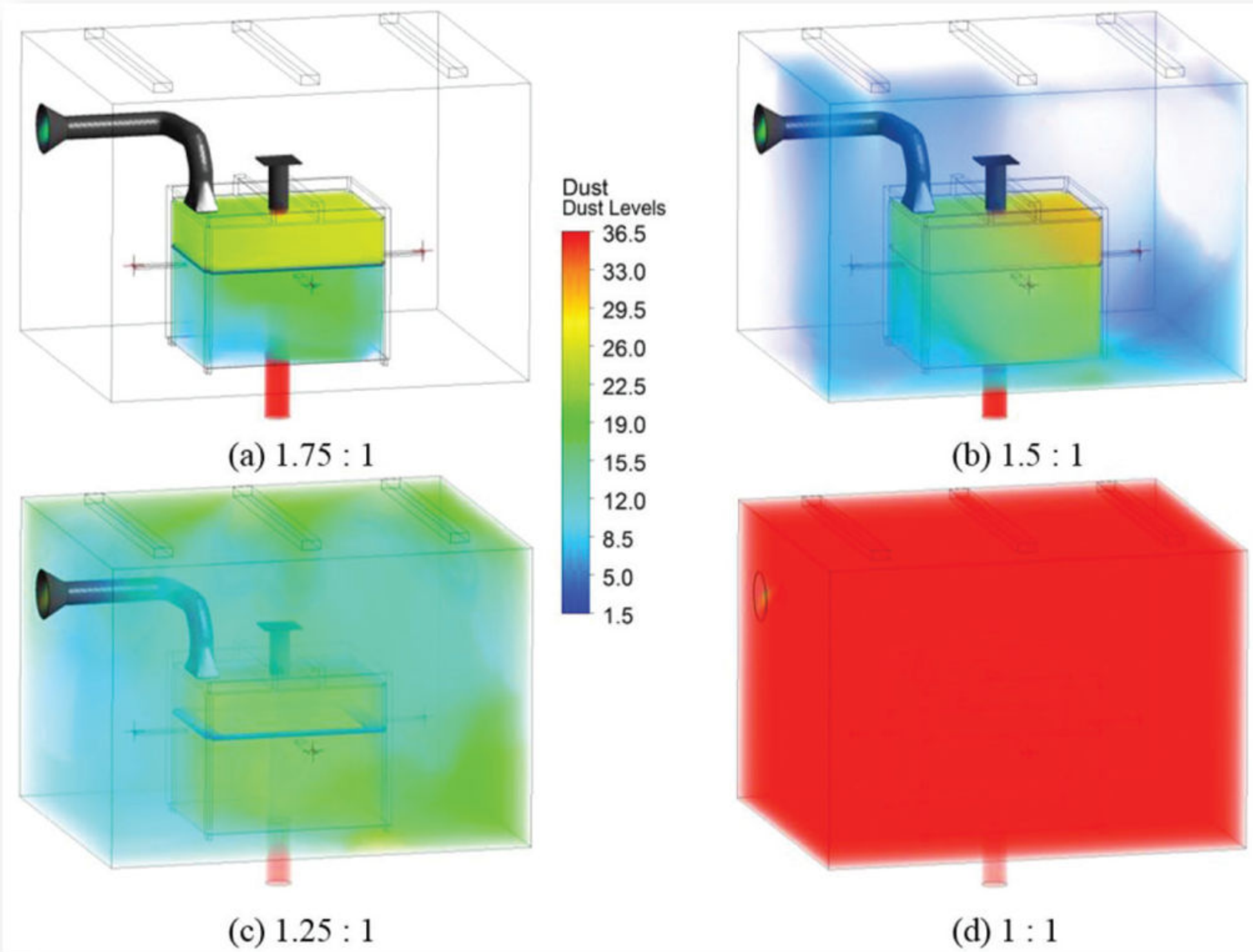

Figure 7.
Respirable dust concentration distributions. Legend shows the dust levels (1.5 to 36.5 mg/m^3) with a 15.2-cm (6-in.)-wide air-blocking shelf for various dust collector-to-bailing airflow ratios: (a) 1.75:1, (b) 1.5:1, (c) 1.25:1 and (d) 1:1.

Table 1

Input parameters for CFD models in drill shroud air-blocking shelf study.

Simulation setups	**Parameter descriptions**
Simulation model	Species transport model without reactions.
Turbulence model	K-epsilon (k-ε), realizable, enhanced wall condition.
Boundary conditions	Roof airflow inlet: velocity inlet (varies according to different collector-to-bailing airflow ratios).
	Dust collector outlet: pressure outlet (0 Pa).
	Bailing air inlet: velocity inlet = 11.438 m/s to provide 0.24 m^3/s (500 cfm) bailing airflow; T = 298.16 K; dust (CO_2) mass fraction = 3.07×10^{-5}
	Others: wall or interior plane.
Solution method	Pressure-velocity coupling scheme: SIMPLE.
	Spatial discretization for gradient: Green-Gauss Node-based method; for pressure: PRESTO method; others: 2nd-order upwind scheme.